IEEE Access
Multidisciplinary ⋮ Rapid Review ⋮ Open Access Journal

Received 6 January 2023, accepted 17 January 2023, date of publication 24 February 2023, date of current version 1 March 2023.

Digital Object Identifier 10.1109/ACCESS.2023.3248604

RESEARCH ARTICLE

An Adaptive Backstepping Sliding-Mode Control for Improving Position Tracking of a Permanent-Magnet Synchronous Motor With a Nonlinear Disturbance Observer

TON HOANG NGUYEN[1], TY TRUNG NGUYEN[1], KIEN MINH LE[2], HOANG NGOC TRAN[3], AND JAE WOOK JEON[1], (Senior Member, IEEE)

[1]Department of Electrical and Computer Engineering, Sungkyunkwan University, Suwon 16419, South Korea
[2]Faculty of Control Engineering, Le Quy Don Technical University, Hanoi 11900, Vietnam
[3]Department of Software Engineering, FPT University, Can Tho 94000, Vietnam

Corresponding author: Jae Wook Jeon (jwjeon@skku.edu)

This work was supported by Institute of Information and Communications Technology Planning and Evaluation (IITP) grant funded by the Korea government (MSIT(Ministry of Science and ICT)) (2021-0-01364, An intelligent system for 24/7 real-time traffic surveillance on edge devices).

ABSTRACT To provide reliable position control for a permanent-magnet synchronous motor (PMSM) under conditions of lumped disturbances such as external load torque fluctuation and system parameter variation, an adaptive backstepping sliding-mode control (ABSMC) with a nonlinear disturbance observer (NDO) is proposed. An ABSMC is a non-cascade technique that employs a position-current single-loop control structure rather than a conventional cascade control structure for vector control of the PMSM. This method uses Lyapunov theory to design a control law that ensures the motor position reaches a desired value in a finite period of time and consequently achieves a rapid transient response. The proposed ABSMC incorporates adaptive convergence gain to avoid a large overshoot under point-to-point position command. The NDO with nonlinear observer gain is proposed to estimate unknown disturbances and provide feed-forward compensation for the ABSMC, improving robustness and reducing steady-state position error. The proposed methods are applied to an industrial motor drive to confirm their validity in real-world operating environments.

INDEX TERMS Permanent magnet synchronous motor, position tracking, adaptive backstepping sliding mode control, nonlinear disturbance observer, disturbance.

I. INTRODUCTION

Permanent-magnet synchronous motors (PMSMs) are widely employed in industrial applications, such as robotics, transportation, elevators, and machine tools, due to their compact construction, high power density, high performance, and low losses [1], [2]. Field-oriented control is a popular technique for high-performance motor drive control. Field-oriented control-based cascade proportional integral derivative (PID) control is a commonly used and effective linear technique for regulating PMSMs [3] thanks to its simplicity and overall performance at certain operating points. However, as a nonlinear system, PMSM is often distorted by nonlinearities, parameter uncertainties, and external disturbances when operating under various conditions that can cause undesirable dynamic responses in the motor [4]. In such cases, it may not be possible to guarantee the overall performance of the motor system using conventional linear feedback control. An alternative method is therefore needed to maintain the high dynamic performance of the motor drive. Several nonlinear techniques have been developed to improve the control performance of motor systems, including backstepping control [5], [6], [7],

The associate editor coordinating the review of this manuscript and approving it for publication was Jinquan Xu.

adaptive control [8], [9], fuzzy-logic control [10], [11], sliding mode control (SMC) [12], [13], [14], [15], [16], [17], and model predictive control [18], [19], [20].

Among these methods, backstepping control is a systematic and recursive approach to nonlinear systems based on Lyapunov stability theory, which ensures global asymptotic stability [21]. This method can transform complex nonlinear control systems into simple reduced-order subsystems [6]. A control law for motor position tracking or speed regulation can be derived through recursive design and virtual control variables. However, backstepping is model-based and cannot ensure the robustness of PMSM drives in the presence of uncertainties and external disturbances [5]. To overcome this limitation, a robust backstepping tracking controller with a load torque observer has been developed using PMSM machine parameter data [22] to provide precise control of the reference trajectory. Tan et al. [23] has also developed an adaptive integrated backstepping approach with a friction compensator to compensate for unknown system parameters and disturbances to a certain extent.

Extensive research has shown SMCs to be useful in industrial applications [24], [25] because of their robustness to disturbances, rapid response time, and ease of implementation. However, to guarantee the robustness of an SMC under parameter uncertainties and external disturbances, switching gain larger than the upper bound of the lumped disturbance is often required, leading to undesirable chattering phenomena [26]. Several approaches have been proposed to overcome the chattering, including a boundary layer approach [27], high-order SMC [28], fuzzy sliding-mode method [10], terminal SMC [29], and a reaching law method [15], [26]. Among these approaches, the reaching law has proven to be an effective strategy for reducing chattering. It directly affects the reaching process by modifying the control gain functions that satisfy the requirements for robustness and reduction in chattering. The control gain has a potentially large value during the reaching phase, while its value will be small during the sliding phase. Therefore, robustness near the sliding-mode surface decreases when an external disturbance occurs [12]. The combination of an SMC with a disturbance observer is an attractive method to improve the robustness of the SMC-based reaching law method. A disturbance observer can estimate an unknown disturbance (including parameter variations and external disturbances) and feed it forward to the SMC. Therefore, the switching gain only needs to be greater than the estimation error [30], which is much smaller than the upper bound of the lumped disturbance, to reduce the chattering.

The disturbance observer is an essential part of the motor controller, as uncertainties and external disturbances are inevitable in motors. Several disturbance observer approaches, such as the Luenberger observer [10], [15], the sliding-mode observer [26], [31], the finite-time disturbance compensator [32], and the extended-state observer [22], [24] have been proposed to estimate and compensate for unknown disturbances in practical applications. Experimental results indicate that the disturbance can be mitigated from the output by feeding the estimated disturbance forward to the controller without affecting system performance. Nonlinear disturbance observer (NDO) control methods [33], [34], [35] have recently been studied because they are easy to implement and produce reliable disturbance estimates. This technique has been tested on robots, converters, and motor drives, with the results demonstrating that highly robust performance is achievable [4]. However, such research used a fixed observer gain for the NDO, which may cause the observer to provide a slower convergence rate in certain critical scenarios, such as a sudden change in external load torque [36].

The main goal of this paper is to propose a controller for position tracking to enhance the overall performance of the PMSM control system through rapid transient response, small steady-state position error, reduced overshoot, and robustness against unknown disturbances. Inspired by a composite method that combines the advantages of backstepping control and SMC for PMSM speed regulation [5], this paper extends the concept to a backstepping sliding-mode control (BSMC) for position tracking. However, a BSMC can cause large overshoots in position step profiles due to the fixed convergence gain of the backstepping method. To address this problem, an adaptive BSMC (ABSMC) that contains an adaptive convergence gain is proposed. Using the proposed method, it is possible to both accelerate the actual position toward the target position and reduce overshoot. In addition, by improving the nonlinear observer gain function of the NDO, parameter uncertainties and external load torque disturbances can be observed and provided with feed-forward compensation to the ABSMC, preserving the robustness of the ABSMC and reducing steady-state error. The primary contributions to this article are:

1) A position-current single-loop control structure simplifies conventional cascade position controller structures by incorporating both backstepping control and SMC. The composite ABSMC offers the asymptotic stability of backstepping control and the robustness and rapid convergence of SMC. The ABSMC also contains an adaptive law for adjusting backstepping convergence gain, which can be used to avoid large overshoots under point-to-point position command.
2) To improve the disturbance rejection and robustness of the ABSMC, an NDO with an improved nonlinear observer gain function is used to enhance robustness and reduce chattering and steady-state position error.
3) The proposed method was implemented on an industrial motor driver and compared with PID [37], SMC [13], a super-twisting-like fractional (STLF) controller [16], and a non-singular fast terminal sliding mode controller (NFTSMC) [17]. Comparative and extensive experiments demonstrate that the proposed method has a rapid transient response, low steady-state

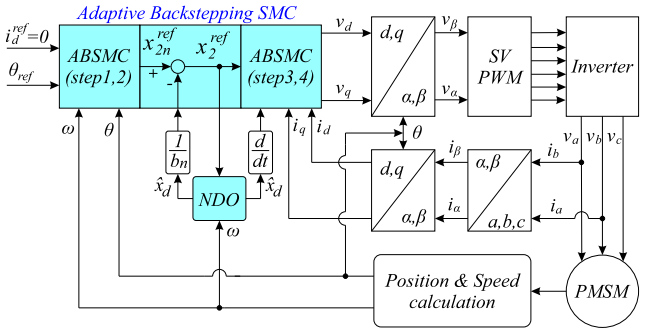

FIGURE 1. Non-cascade structure for position control of the proposed ABSMC+NDO.

position error and reduced overshoot, and is robust to external load and parameter disturbances.

The rest of this article is constructed as follows. The mathematical formulation of a PMSM is introduced in Section II. Position control based on a BSMC scheme is detailed in Section III. Section IV addresses disturbance rejection based on the NDO and presents a combination of the BSMC and NDO. In Section V, an adaptive rule for convergence gain for the BSMC that eliminates the large overshoot when operating with step-position commands is discussed. Section VI explores the experimental results, and a conclusion is presented in Section VII.

II. MATHEMATICAL MODEL OF THE PMSM

In this paper, a non-cascade control method is proposed to improve the position tracking performance of PMSM drivers (Fig. 1). This method employs an ABSMC to design the current controller for the q and d axes, providing voltage supplies (v_q and v_d) for the motor. The ABSMC is a combination of backstepping and SMC control, where the backstepping component includes an adaptive convergence gain to avoid large overshoots. Moreover, to mitigate the impact of uncertainty parameters and external disturbances, the NDO [38], [39] is utilized with some modifications to the observer gain design. This helps estimate the unknown disturbance and feed it forward to the ABSMC, ensuring the robustness of the motor system. The mathematical model of the PMSM system in the rotor $d-q$ reference frame can be expressed as [3]:

$$\frac{di_d}{dt} = \frac{1}{L_d}(-Ri_d + P\omega L_q i_q + v_d) \tag{1}$$

$$\frac{di_q}{dt} = \frac{1}{L_q}(-Ri_q - P\omega L_d i_d - P\omega\Phi + v_q) \tag{2}$$

$$T_e = 1.5P[\Phi i_q + (L_d - L_q)i_d i_q] \tag{3}$$

where i_d and v_d are the stator current and voltage in the $d-$axis, while i_q and v_q are the stator current and voltage in the $q-$axis, respectively. R is the stator resistance, L_d and L_q are the stator inductances in the $d-q$ frame, P is the number of rotor pole pairs, Φ is the flux linkage of the rotor permanent magnets, ω is the angular velocity of the rotor, and T_e is the electromagnetic torque. To provide a constant flux condition in the PMSM, the $d-$axis reference was set to zero and the inductances in $d-$ and $q-$axes were considered equal $L_d = L_q$ [40]. The electromagnetic torque, T_e, is dependent solely on the $q-$axis current and can be expressed as follows:

$$T_e = 1.5P\Phi i_q = K_t.i_q \tag{4}$$

where K_t is the torque constant. The motion equation of the motor can be expressed as:

$$\frac{d\theta}{dt} = \omega \tag{5}$$

$$T_e = J\frac{d\omega}{dt} + B\omega + T_L \tag{6}$$

where θ represents the position angle of the rotor, J refers to the total moment of inertia (which includes both the rotor and load), B represents the frictional coefficient, and T_L represents the external load torque, which is assumed to be unknown but varies slowly within a small sampling interval. In practical operating conditions, the motor can often be affected by both variations in internal parameters and external disturbances. According to equation (6), the mechanical equation can be rewritten as follows

$$T_e = J_n\frac{d\omega}{dt} + B_n\omega + d \tag{7}$$

where J_n and B_n are the nominal values of J and B, respectively, with $J = J_n + \Delta J$ and $B = B_n + \Delta B$. The value of d is defined as $d = (\Delta J\frac{d\omega}{dt} + \Delta B\omega + T_L)$, which contains internal parameter variations and external load torque. These are considered as lumped disturbances in the motor. The value of d is unknown, causing an undesired dynamic response.

Assumptions : 1) The lumped disturbances do not have an excessive effect on the system, and they are bound (i.e., $|d| < D_1$ with $D_1 > 0$) and vary slowly during a small sampling interval in the actual system. 2) The disturbance derivative will also be bound in the controller (i.e., there exists $D_2 > 0$ such that $|\dot{d}| < D_2$).

The main purpose of this study was to construct a position controller that improves the position tracking of the motor. First, a BSMC was designed to replace the conventional position control based on a cascade control structure. Then a NDO was used with a modified observer gain function to improve robustness and reduce steady-state error in position tracking. However, because the backstepping in the BSMC used fixed convergence gains, a large overshoot occurred in the position step profile. To address this problem, an adaptive convergence gain for the backstepping was proposed.

III. DESIGN OF THE BSMC FOR POSITION CONTROLLER

The BSMC for position control is described first in this section. The drawbacks of the BSMC are then analyzed, and the design of the proposed ABSMC is described in Section V. To facilitate the controller design, equations (5), (7), (2),

and (1) are collected and rewritten as (8)–(11), respectively:

$$\dot{x}_0 = x_1 \tag{8}$$
$$\dot{x}_1 = -a_n x_1 + b_n x_2 + x_d \tag{9}$$
$$\dot{x}_2 = f_q(x) + b_2 v_q \tag{10}$$
$$\dot{x}_3 = f_d(x) + b_3 v_d \tag{11}$$

where $x_0 = \theta$, $x_1 = \omega$, $x_2 = i_q$ and $x_3 = i_d$ are the measurable variables; $x_d = -d/J_n$ is lumped disturbance and unknown; and $a_n = B_n/J_n$, $b_n = K_t/J_n$, $f_q(x) = \frac{-1}{L_q}(Ri_q + P\omega L_d i_d + \frac{2}{3}K_t\omega)$, $b_2 = 1/L_q$; $f_d(x) = \frac{1}{L_d}(P\omega L_q i_q - Ri_d)$ and $b_3 = 1/L_d$. Equations (8)-(10) were used to construct the $q-$axis current controller (Steps 1 to 3 in Fig. 1), and equation (11) was used to construct the $d-$axis current controller (Step 4 in Fig. 1).

A. Q-AXIS CURRENT CONTROLLER DESIGN

The position controller is designed to keep the actual motor position θ tracking the reference position $x_0^{ref} = \theta^{ref}$ accurately under any variation in internal parameters and external disturbances. To achieve this control aim, the position error $e_0 = x_0^{ref} - x_0$ should be minimized. The main idea of backstepping control is to reduce a high-order system into several first-order subsystems by providing virtual control variables [6]. The control law is designed based on the Lyapunov stability theory.

Step 1: Select a candidate Lyapunov function as $V_0 = 0.5\, e_0^2$, then take the derivative of V_0 with respect to time:

$$\dot{V}_0 = e_0\dot{e}_0 = e_0(\dot{x}_0^{ref} - \dot{x}_0) = e_0(\dot{x}_0^{ref} - x_1) \tag{12}$$

From (12), the virtual control input for the (9) is designed as:

$$x_1^{ref} = \dot{x}_0^{ref} + c_0 e_0 \tag{13}$$

where $c_0 > 0$ is a strictly positive constant for an asymptotic rate of convergence.

Step 2: Based on the value x_1^{ref} from Step 1, the difference between x_1^{ref} and x_1 is $e_1 = x_1^{ref} - x_1$. The second Lyapunov function is selected as $V_1 = V_0 + 0.5e_1^2$. The time derivative of V_1 is obtained as

$$\begin{aligned}\dot{V}_1 &= \dot{V}_0 + e_1\dot{e}_1 = e_0(\dot{x}_0^{ref} - x_1) + e_1\dot{e}_1 \\ &= e_0(\dot{x}_0^{ref} + e_1 - x_1^{ref}) + e_1\dot{e}_1 \\ &= e_0(e_1 - c_0 e_0) + e_1\dot{e}_1 = -c_0 e_0^2 + e_1(e_0 + \dot{e}_1)\end{aligned} \tag{14}$$

From (13) and (9), the term $\dot{e}_1$ is determined by

$$\begin{aligned}\dot{e}_1 &= \dot{x}_1^{ref} - \dot{x}_1 \\ &= \ddot{x}_0^{ref} + c_0(\dot{x}_0^{ref} - x_1) + a_n x_1 - b_n x_2 - x_d\end{aligned} \tag{15}$$

From (14) and (15), the term $e_0 + \dot{e}_1$ is designed to equal $-c_1 e_1$:

$$e_0 + \ddot{x}_0^{ref} + c_0(\dot{x}_0^{ref} - x_1) + a_n x_1 - b_n x_2 - x_d = -c_1 e_1 \tag{16}$$

The virtual control input for the (10) can then be determined as

$$x_2^{ref} = x_{2n}^{ref} - \frac{x_d}{b_n} \tag{17}$$

where x_{2n}^{ref} is the nominal virtual control signal without considering the uncertainties and external load torque:

$$\begin{aligned}x_{2n}^{ref} &= \frac{1}{b_n}[e_0 + \ddot{x}_0^{ref} + c_0(\dot{x}_0^{ref} - x_1) + a_n x_1 + c_1 e_1] \\ &= \frac{1}{b_n}[\ddot{x}_0^{ref} + a_n x_1 + (c_0 + c_1)\dot{e}_0 + (c_0 c_1 + 1)e_0]\end{aligned} \tag{18}$$

The virtual control signal x_2^{ref} contains the lumped disturbance x_d, which will cause an undesirable response in the motor system. To overcome the negative effect of the disturbance on the controller, a NDO was designed to estimate and compensate for it in Section IV.

The positive gains c_0 and c_1 in (13) and (18) represent the convergence gain of the backstepping controller. If these gains are large, the system will have a faster response and superior robustness, but a large overshoot will occur in the step profile. If the value of these gains is small, the system will respond slowly, and the overshoot will be reduced. There is therefore a trade-off between settling time and overshoot. This problem will be addressed in Section V.

Step 3: Based on the value x_2^{ref} from Step 2, the difference between x_2^{ref} and x_2 is $e_2 = x_2^{ref} - x_2$. In this step, a SMC is used to design the voltage supply v_q for the motor, and the procedure is separated into two parts: designing the sliding-mode surface and the reaching law. First, the sliding-mode surface is designed based on error e_2:

$$S_1 = e_2 \tag{19}$$

Considering the Lyapunov function $V_2 = V_1 + 0.5\, S_1^2$, the differential of V_2 with respect to time becomes:

$$\begin{aligned}\dot{V}_2 &= e_0\dot{e}_0 + e_1\dot{e}_1 + S_1\dot{S}_1 \\ &= e_0(e_1 - c_0 e_0) + e_1(\dot{x}_1^{ref} - \dot{x}_1) + S_1\dot{S}_1\end{aligned} \tag{20}$$

From (17) and (18), the term $(\dot{x}_1^{ref} - \dot{x}_1)$ is calculated as

$$\begin{aligned}\dot{x}_1^{ref} - \dot{x}_1 &= \dot{x}_1^{ref} + a_n x_1 - b_n x_2 - x_d \\ &= \dot{x}_1^{ref} + a_n x_1 - b_n(x_2^{ref} - e_2) - x_d \\ &= \dot{x}_1^{ref} + a_n x_1 - b_n x_{2n}^{ref} + b_n e_2 \\ &= -e_0 - c_1 e_1 + b_n e_2\end{aligned} \tag{21}$$

Substitute (21) into (20), the $\dot{V}_2$ can be rewritten as

$$\dot{V}_2 = -c_0 e_0^2 - c_1 e_1^2 + b_n e_1 e_2 + S_1\dot{S}_1 \tag{22}$$

The constant-proportional rate reaching law [13] for the sliding mode is designed as below

$$\dot{S}_1 = -k_1 sgn(S_1) - k_2 S_1 - b_n e_1; \quad k_1, k_2 > 0 \tag{23}$$

The resulting control system is therefore asymptotically stable $\dot{V}_2 = -c_0 e_0^2 - c_1 e_1^2 - k_1 S_1 sgn(S_1) - k_2 S_1^2 \leq 0$.

The derivative with respect to time of S_1 is:

$$\dot{S}_1 = \dot{e}_2 = \dot{x}_2^{ref} - \dot{x}_2 = \dot{x}_{2n}^{ref} - \frac{\dot{x}_d}{b_n} - \dot{x}_2 \tag{24}$$

with

$$\dot{x}_{2n}^{ref} = b_n^{-1}[\dot{e}_0 + \dddot{x}_0^{ref} + c_0\ddot{x}_0^{ref} + (a_n - c_0)\dot{x}_1 + c_1\dot{e}_1] \tag{25}$$

Substituting (15) and (9) into (25) yields:

$$\dot{x}_{2n}^{ref} = h_q(x) - k_{ac}x_d \tag{26}$$

where $h_q(x) = b_n^{-1}[\dddot{x}_0^{ref} + (c_0 + c_1)\ddot{x}_0^{ref} + (c_0c_1 + 1)(\dot{x}_0^{ref} - x_1) - (c_0 + c_1 - a_n)(-a_nx_1 + b_nx_2)]$, and $k_{ac} = (c_0 + c_1 - a_n)b_n^{-1}$.

From (10), (23), (24) and (26) the $\dot{S}_1$ is derived

$$\begin{aligned}\dot{e}_2 &= h_q(x) - k_{ac}x_d - \frac{\dot{x}_d}{b_n} - f_q(x) - b_2v_q \\ &= -k_1sgn(S_1) - k_2S_1 - b_ne_1\end{aligned} \tag{27}$$

From the above equation, the voltage supply for the $q-$axis can be derived as

$$\begin{aligned}v_q = b_2^{-1}[&h_q(x) - k_{ac}x_d - \frac{\dot{x}_d}{b_n} - f_q(x) \\ &+k_1sgn(S_1) + k_2S_1 + b_ne_1]\end{aligned} \tag{28}$$

From equation (28), it can be seen that the control signal v_q contains the terms x_d and its derivative $\dot{x}_d$. The design of v_q is therefore not complete. To overcome this problem, the lumped disturbance is considered in Section IV.

B. D-AXIS CURRENT CONTROLLER DESIGN

Step 4: This step designs the control signal v_d to make the $d-$axis current output from the motor track the reference current $i_d^{ref} = x_3^{ref}$ (as mentioned above, $i_d^{ref} = 0$ to provide a constant flux). To achieve this goal, the difference $e_3 = 0 - x_3$ should be minimized. As in Step 3, the SMC is used to design the control signal v_d. The sliding surface is designed with:

$$S_2 = e_3 + \alpha_1\int_0^t e_3(\tau)\,d\tau \tag{29}$$

where $\alpha_1 > 0$, and the control signal v_d is derived using the reaching law [13]:

$$\dot{S}_2 = -k_3sgn(S_2) - k_4S_2; \quad k_3, k_4 > 0 \tag{30}$$

From (29), taking the derivative of S_2 yields:

$$\dot{S}_2 = \dot{e}_3 + \alpha_1e_3 = -f_d(x) - b_3v_d + \alpha_1e_3 \tag{31}$$

From (30) and (31), the control signal v_d can be calculated:

$$v_d = b_3^{-1}[-f_d(x) + \alpha_1e_3 + k_3sgn(S_2) + k_4S_2] \tag{32}$$

Defining the Lyapunov function $V_3 = 0.5S_2^2$. Then $\dot{V}_3 = S_2\dot{S}_2 = -k_3S_2sgn(S_2) - k_4S_2^2 \leq 0$ can be ensured. The value of x_3 will therefore converge to 0.

IV. DESIGN OF THE NONLINEAR DISTURBANCE OBSERVER AND PROOF OF SYSTEM STABILITY

A. DESIGN OF THE NONLINEAR DISTURBANCE OBSERVER

From the virtual control input x_2^{ref} in (17) and the control law for the voltage supply v_q in (28), the lumped disturbance, x_d, and its first derivative term, $\dot{x}_d$, will cause an undesirable dynamic. Although it is possible to compensate for a lumped disturbance and retain a certain level of robustness by designing a large sliding-mode switching gain (k_1 and k_2), this can cause significant chattering, and fail to provide an effective dynamic response in some applications [26]. An alternative solution is to design a disturbance observer to estimate the lumped disturbance and feed it forward to the control law online.

Considering the subsystem (9) contained uncertainty and external disturbances with the virtual control x_2^{ref} that was obtained from step 2

$$\dot{x}_1 = -a_nx_1 + b_nx_2^{ref} + x_d \tag{33}$$

The NDO [38], [39] is designed as:

$$\begin{aligned}\dot{\hat{x}}_d &= l(x_1)[x_d - \hat{x}_d] \\ &= l(x_1)[\dot{x}_1 + a_nx_1 - b_nx_2^{ref} - \hat{x}_d]\end{aligned} \tag{34}$$

where $l(x_1) > 0$ represents the observer gain. As the state $\dot{x}_1$ cannot be measured directly, the preceding equation was rewritten as:

$$\dot{\hat{x}}_d - l(x_1)\dot{x}_1 = l(x_1)[a_nx_1 - b_nx_2^{ref} - \hat{x}_d] \tag{35}$$

An internal state z is defined such that

$$\dot{z} = \dot{\hat{x}}_d - l(x)\dot{x}_1 \tag{36}$$

and a nonlinear function $p(x_1)$ with a derivative with respect to x_1 equal to $l(x_1)$, so that $\frac{\partial p(x_1)}{\partial x_1} = l(x_1)$. Integrating (36) with respect to time yields $z = \hat{x}_d - p(x_1)$, and the lumped disturbance $\hat{x}_d$ can be estimated

$$\hat{x}_d = z + p(x_1) \tag{37}$$

From (35), (36) and (37) the $\dot{z}$ can be calculated as

$$\dot{z} = l(x_1)[a_nx_1 - b_nx_2^{ref} - (z + p(x_1))] \tag{38}$$

Considering the observer error $e_d = x_d - \hat{x}_d$, the $\dot{e}_d$ is obtained:

$$\dot{e}_d = \dot{x}_d - \dot{\hat{x}}_d = \dot{x}_d - l(x_1)[x_d - \hat{x}_d] = \dot{x}_d - l(x_1)e_d \tag{39}$$

For a simple design [33], [34], [35], the observer gain is commonly selected to be a fixed constant value $L_1 > 0$, and the function $p(x_1) = L_1x_1$ becomes a linear function to estimate the disturbance. As a result, the disturbance observer can be referred to as a linear disturbance observer (LDO) when using a constant observer gain. The derivative of observer error becomes $\dot{e}_d = \dot{x}_d - L_1e_d$. It follows that the observer error can be obtained by [36]:

$$|e_d(t)| \leq |e_d(0)|e^{-L_1t} + \frac{\varepsilon}{L_1} \tag{40}$$

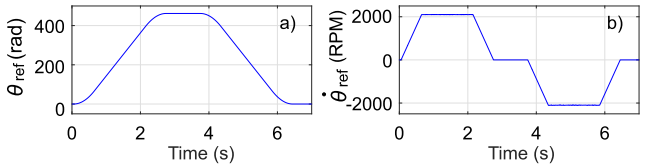

FIGURE 2. Trapezoidal velocity motion profile. (a) Position profile θ_{ref}. (b) Velocity profile $\dot{\theta}_{ref}$.

where $|\dot{x}_d| < \varepsilon$, with $\varepsilon > 0$ is the bound of derivative of the lumped disturbance x_d.

From equation (40), in the case when the system experiences a constant lumped disturbance, $\dot{x}_d = 0$, meaning $\varepsilon = 0$, the observer error, e_d, will converge to zero. This implies that the disturbance observer can accurately estimate the lumped disturbance in the steady state. When the lumped disturbance changes slowly and its derivative is bounded by ε, the observer error (40) is asymptotically and exponentially stable for the initial error, $e_d(0)$. However, a steady state error, ε/L_1, still exists, and depends on the value of L_1. Increasing the magnitude of the observer gain decreases the observer error, e_d, and leads to a faster disturbance estimation response. However, a fixed observer gain may result in a slower convergence rate in critical scenarios, such as sudden changes in external load torque [36]. To address this issue, we propose a nonlinear design function, $p(x_1)$, referred to as the NDO:

$$p(x_1) = L_1 x_1 + L_2 x_1^2 sgn(x_1) \tag{41}$$

where L_1 and $L_2 > 0$ are constant parameters. In contrast to the fixed gain designed in [33], [34], and [35], the proposed NDO employs a nonlinear design function $p(x_1)$, which combines first- and second-order state variables. Differentiating the nonlinear function $p(x_1)$ with respect to x_1 yields:

$$l(x_1) = L_1 + 2L_2 x_1 sgn(x_1) \geq L_1 \tag{42}$$

The observer gain $l(x_1)$ is constructed to meet the condition of globally exponential stability [39] of the observer error in (39). It is clear that the proposed $l(x_1)$ has a larger magnitude when compared with the constant gain L_1, which is used in [33], [34], and [35]. As a result, the nonlinear gain $l(x_1)$ can provide a faster convergence rate while also reducing observer error.

Fig. 3 shows the results of the NDO and LDO when combined with the (A)BSMC under trapezoidal velocity motion profiles (Fig. 2). The term (A)BSMC means that the ABSMC and BSMC performed similarly under trapezoidal velocity motion profiles. The main advantage of the ABSMC is the reduction of overshoot under the step position profile, which will be demonstrated later. Fig. 3(a) and (b) show the position error of the (A)BSMC+NDO and (A)BSMC+LDO. The NDO, using the proposed nonlinear observer gain function (41), achieved a steady state position error of 0.0009 rad, outperforming the LDO result of 0.0016 rad.

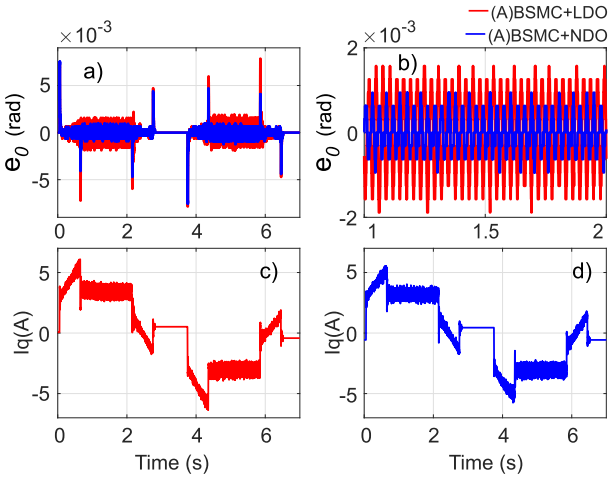

FIGURE 3. Experimental results of (A)BSMC+LDO and (A)BSMC+NDO under a trapezoidal velocity motion profile, the steady-state speed is ±2100 rpm. (a) and (b) Position error. (c) and (d) $q-$axis current of the (A)BSMC+LDO and (A)BSMC+NDO.

B. PROOF OF THE SYSTEM STABILITY

Through the design of the $d-$axis current controller, it can be seen that the $d-$axis control system is stable; $\dot{V}_3 \leq 0$. To design the $q-$axis current controller, considering the motor system (9) with the lumped disturbance x_d, the NDO is employed to estimate the lumped disturbance and provide a feed-forward combination for the control law in the control signal (Fig. 1). The control signals x_2^{ref} and v_q can be expressed as

$$x_2^{ref} = x_{2n}^{ref} - \frac{\hat{x}_d}{b_n} \tag{43}$$

$$v_q = b_2^{-1}[h_q(x) - k_{ac}\hat{x}_d - \frac{\dot{\hat{x}}_d}{b_n} - f_q(x) + b_n e_1 + k_1 sgn(S_1) + k_2 S_1] \tag{44}$$

Define the Lyapunov function $V = V_2 + V_3$. Taking the derivative of V and combining (20) and $\dot{V}_3$:

$$\dot{V} = e_0(e_1 - c_0 e_0) + e_1(\dot{x}_1^{ref} - \dot{x}_1) + S_1\dot{S}_1 - k_3 S_2 sgn(S_2) - k_4 S_2^2 \tag{45}$$

The term $(\dot{x}_1^{ref} - \dot{x}_1)$ is calculated by using (43), (13), and (18):

$$\begin{aligned} \dot{x}_1^{ref} - \dot{x}_1 &= \dot{x}_1^{ref} + a_n x_1 - b_n(x_2^{ref} - e_2) - x_d \\ &= \dot{x}_1^{ref} + a_n x_1 - b_n x_{2n}^{ref} + b_n e_2 - e_d \\ &= -e_0 - c_1 e_1 + b_n e_2 - e_d \end{aligned} \tag{46}$$

The derivative with respect to time of S_1 is calculated by using (44), (26), and (10):

$$\begin{aligned} \dot{S}_1 = \dot{e}_2 &= \dot{x}_2^{ref} - \dot{x}_2 = \dot{x}_{2n}^{ref} - \frac{\dot{\hat{x}}_d}{b_n} - \dot{x}_2 \\ &= h_q(x) - k_{ac}x_d - \frac{\dot{\hat{x}}_d}{b_n} - f_q(x) - b_2 v_q \\ &= -b_n e_1 - k_1 sgn(S_1) - k_2 S_1 - k_{ac} e_d \end{aligned} \tag{47}$$

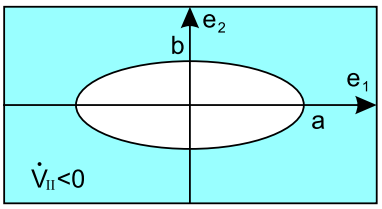

FIGURE 4. Region of $\dot{V}_{II} < 0$.

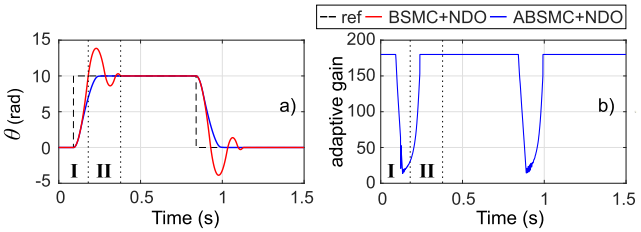

FIGURE 5. Experimental results of BSMC+NDO and the proposed ABSMC+NDO under point-to-point profile (step change 10*rad*). (a) Position tracking. (b) Adaptive convergence gain.

Substituting (46) and (47) into (45) yields:

$$\dot{V} = \dot{V}_I + \dot{V}_{II} \tag{48}$$

where $\dot{V}_I = -c_0 e_0^2 - k_3 S_2 sgn(S_2) - k_4 S_2^2 - k_1 S_1 sgn(S_1) \leq 0$, and

$$\begin{aligned} \dot{V}_{II} &= -c_1 e_1^2 - k_2 S_1^2 - e_d e_1 - k_{ac} e_d e_2 \\ &\leq -c_1 e_1^2 - k_2 S_1^2 + \frac{\varepsilon}{L_1}|e_1| + k_{ac}\frac{\varepsilon}{L_1}|e_2| \end{aligned} \tag{49}$$

where $k_{ac} > 0$, then $c_0 + c_1 > a_n$. Since

$$\frac{\varepsilon}{L_1}|e_1| + k_{ac}\frac{\varepsilon}{L_1}|e_2| \leq \frac{\varepsilon^2}{L_1^2 c_1} + \frac{c_1}{4}e_1^2 + \frac{k_{ac}^2\varepsilon^2}{L_1^2 k_2} + \frac{k_2}{4}e_2^2 \tag{50}$$

by Young's inequality, it follows that

$$\begin{aligned} \dot{V}_{II} &\leq -\frac{3}{4}c_1 e_1^2 - \frac{3}{4}k_2 e_2^2 + \frac{\varepsilon^2}{L_1^2 c_1 k_2}(k_2 + c_1 k_{ac}^2) \\ &\leq -M[\frac{e_1^2}{a^2} + \frac{e_2^2}{b^2} - 1] \end{aligned} \tag{51}$$

where $M = \frac{\varepsilon^2}{L_1^2 c_1 k_2}(k_2 + c_1 k_{ac}^2)$, $a = \frac{\varepsilon}{L_1 c_1}\sqrt{\frac{k_2 + c_1 k_{ac}^2}{0.75 k_2}}$, and $b = \frac{\varepsilon}{L_1 k_2}\sqrt{\frac{k_2 + c_1 k_{ac}^2}{0.75\ c_1}}$. As shown in Fig. 4, the $\dot{V}_{II} < 0$ outside of an ellipse. Since the size of the ellipse can be made arbitrarily small by taking a sufficiently large observer gain L_1 and suitable values of c_1 and k_2, $\dot{V}_{II}(e_1(t), e_2(t))$ tends to an arbitrarily small number as time increases. The robustness of the BSMC+NDO can therefore be maintained.

V. ADAPTIVE BACKSTEPPING SLIDING MODE CONTROL

As mentioned previously, the proposed BSMC contains convergence gains c_0 and c_1 for calculating the virtual control

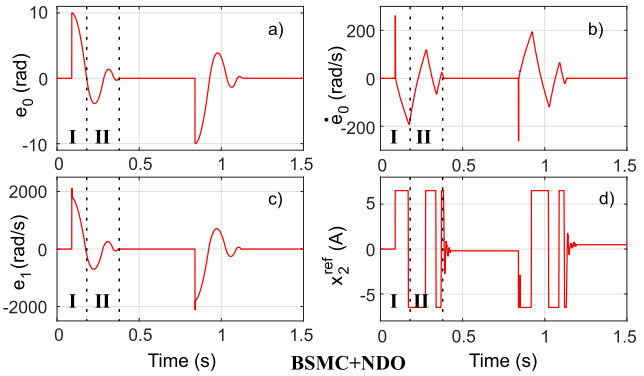

FIGURE 6. Experimental results of the BSMC+NDO under point-to-point profile (step change 10*rad*) corresponding to Fig. 5(a).

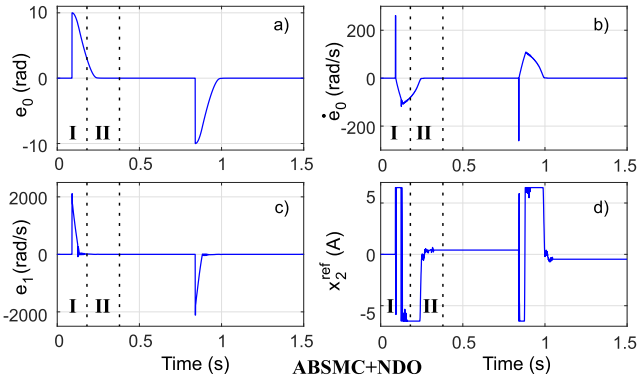

FIGURE 7. Experimental results of the ABSMC+NDO under a point-to-point profile (step change 10*rad*) corresponding to Fig. 5(a).

inputs x_2^{ref} as (18). Based on experiments, c_0 was selected to equal c_1 to obtain reliable control performance. However, the BSMC poses a problem with respect to practical applicability. If these gains are small, the system will respond slowly, and the overshoot will be small. If the gains are large, the system will have a faster response and superior robustness, but a large overshoot will occur in position step profile.

Because of the large changes in the step profile, excessively large errors (e_0 and e_1) occur. As described in (18), these errors will be multiplied by large constant gains (c_0 and c_1), resulting in a large control signal x_2^{ref}. Due to limitations in the physical system, the current is always constrained within a specific range of values. As a result, control saturation occurs, leading to an overshoot in the position response. To tackle this problem, an ABSMC was proposed. The experimental results of the BSMC under the step position command are shown in Figs. 5(a) and Fig. 6. The red line in Fig. 5(a) shows the position response of the BSMC, while Fig. 6 shows the e_0, e_1, $\dot{e}_0$, and the virtual control x_2^{ref}. As can be seen in region I of Fig. 6(a) and (c), the errors e_0 and e_1 are excessively large under the step profile. These errors, when multiplied with the large constant gains of c_0 and c_1, will cause an excessively large virtual control signal x_2^{ref}. Because of the control saturation phenomenon, the actual position increases rapidly from 0 rad and crosses over the reference constant

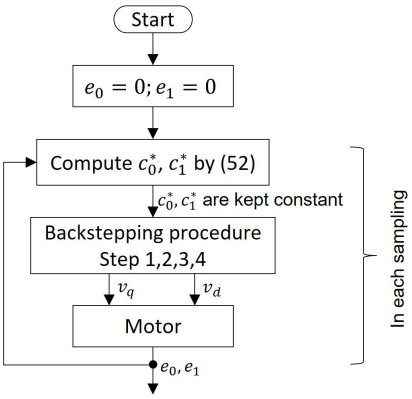

FIGURE 8. Design of adaptive backstepping sliding mode control for position controller.

position of 10 rad in 0.18 s at the end of region I, as shown in Fig. 5(a). The values of e_0 and e_1 are small at the end of region I, but the large gains (c_0, c_1), and the large value of $\dot{e}_0$ in the term $(c_0 + c_1)\dot{e}_0$, which is contained in (18), will continue to produce a large control signal x_2^{ref} in region II, as shown in Fig. 6(d). This results in an overshoot of 38% in the position in Fig. 5(a). Therefore, when excessively large errors occur, the gains of c_0 and c_1 should be lowered to reduce the excessive control signal. The proposed adaptive gain of c_0^* and c_1^* for the ABSMC which ensures $k_{ac} > 0$ is:

$$\begin{aligned} c_0^* &= \begin{cases} c_0 & \text{if } |e_0 e_1| \le \delta \\ c_0 - |\dot{e}_0|(1 + f(e_0)) & \text{if } |e_0 e_1| > \delta \end{cases} \\ &\text{if } c_0^* < 0.5\, a_n \quad \text{then} \quad c_0^* = 0.5 a_n \\ c_1^* &= c_0^* \end{aligned} \tag{52}$$

with

$$f(e_0) = \lambda e^{-\eta |e_0|^{0.5}} \tag{53}$$

where $\delta > 0$ is the experimentally determined threshold.

It should be noted that the convergence gains c_0^* and c_1^* are calculated independently of the backstepping procedure (steps 1, 2, 3, and 4), and the calculated gains are considered constant values in the backstepping procedure, as shown in Fig. 8.

When an excessively large error occurs (e_0 and e_1 are both large), $|e_0 e_1|$ will also be large. The convergence gains of c_0 and c_1 should then be lowered to reduce overshoot. Because the derivative of e_0 indicates how fast the position error e_0 changes in time, it is used to adjust the gain c_0^*. To provide a rapid transient response and reduce overshoot, the gains of c_0 and c_1 should be reasonably adjusted. When an excessively large errors occur, the degree of gain reduction is determined by the magnitude of $\dot{e}_0$ and the exponential function $f(e_0)$ with ($\lambda > 0$ and $\eta > 0$) to appropriately decrease the gain c_0^*.

When the actual position is far from the reference position, e_0 and e_1 are excessively large, and the magnitude of $\dot{e}_0$ tends to increase from a small to a large value, corresponding to region I (Fig. 5). If the gain of c_0^* is immediately changed to a small value at the beginning of region I, the controller will exhibit a slow transient response. As a result, when e_0 is large, $f(e_0)$ should converge to a small value, gradually reducing the gain $c_0^* \approx c_0 - |\dot{e}_0|$ and accelerating the actual position to the reference position. Because of the reduction of the gain of c_0^* to a small value at the end of region I, the excessively large control signal caused by the term $(c_0+c_1)\dot{e}_0$ as analyzed above can be avoided. When the actual position is close to the reference position, e_0 is small, and the magnitude of $\dot{e}_0$ tends to decrease to a small value, corresponding to region II; $f(e_0)$ should therefore converge to λ, forcing the gain $c_0^* \approx c_0 - |\dot{e}_0|(1+\lambda)$ to gradually increase to avoid an excessively large control signal.

The blue line in Figs. 5(a), 5(b), and 7 show the experimental results of the proposed adaptive convergence gain for the ABSMC, demonstrating that the overshoot can be reduced. Fig. 5(b) depicts the adaptive gain, c_0^*, to reduce the overshoot of the proposed ABSMC. When excessive position errors occur due to large changes in the motion profile, the convergence gain c_0^* was adapted to reduce the overshoot. Fig. 7 shows the e_0, e_1, $\dot{e}_0$, and the virtual control signal x_2^{ref} using the proposed ABSMC+NDO. Using the adaptive convergence gain, the excessive control signal x_2^{ref} was reduced at region II, as shown in Fig. 7(d), resulting in the reduced overshoot in Fig. 5(a).

The following statements summarize guidance for selecting control parameters for the proposed control method: The ABSMC has parameters c_0, c_1, k_1, k_2, k_3, k_4, α_1 for the BSMC; and parameters δ, λ, η for the adaptive algorithms, which adjust the convergence gain (c_0, c_1) to reduce overshoot under the position-step profile. For a simple design, c_0 was selected to equal c_1, $k_1 = k_3$, and $k_2 = k_4$. From analysis of system stability (Section IV, $k_{ac} > 0$), the resulting c_0 and c_1 were selected to be larger than 0.5 a_n. If the gains c_0 and c_1 are small, the system will respond slowly, the transient position error will be large, and the overshoot will be small. If these gains are large, the system will have a faster response and superior robustness, but a large overshoot will occur in the step profile. The parameters (k_1, k_2) and (k_3, k_4) are related to SMC for v_q and v_d, under the constant-proportional rates reaching law [13].

To begin, we configured the BSMC parameters by running the motor with a trapezoidal velocity motion profile but without the combination of NDO. The initial values c_0 and c_1 were chosen to be greater than 0.5 a_n. The factors k_1, k_2, k_3, k_4, and α_1 for the constant-proportional rate reaching law [13] were determined according to experimental results such that system chattering would be effectively reduced. We then gradually increased the c_0, c_1 to reduce the transient position error to an acceptable value. After pre-tuning the parameters for BSMC, the NDO was combined with BSMC to reduce the effects of disturbances and uncertainties in the motor system. The transient position error should decrease after adding the

NDO. The observer gain $L_2 = 0$ and L_1 was first selected with a small value and then L_1 was gradually increased to obtain acceptable position error. Similarly, keeping the tuned L_1, we configured L_2 with a small value and gradually increased L_2 to further reduce steady-state position error.

After selecting the parameters for the BSMC and NDO, we operated the motor under the position-step profile to tune the adaptive gain (λ and η) for adjusting the convergence gains c_0 and c_1. By conducting experiments, we realize that the value of λ is in the range [1; 4], η is in the range [0.1; 2] the proposed control method will provide a better result. The threshold δ was configured to begin at a small value and gradually increase to twice the previous value until the overshoot was reduced.

VI. EXPERIMENTAL RESULTS

This section presents experimental results that demonstrate the practicability of the proposed method. The experimental setup and nominal parameters are shown in Fig. 9 and Table 1. The experimental system consists of a PMSM attached to an incremental encoder with 5000 lines, or 20000 pulses per revolution to measure the position and speed of the motor shaft. To test the performance under an external load torque, a ZKG-20AN powder clutch was mounted coaxially to the motor shaft, and a CTA3200 brake controller was used to regulate the current applied to the brake powder to adjust the value of the load torque. An STM32F446VC processor (Cortex-M4, 168Mhz) was integrated into the driver board to implement the proposed method. RS232 communication software was connected to the driver module to record experimental data for debugging and plotting results using the MATLAB software.

The effectiveness of the proposed ABSMC+NDO in this research was compared with the PID [37]+NDO, SMC [13]+NDO, super-twisting-like fractional (STLF) controller [16], and non-singular fast terminal sliding mode controller (NFTSMC) [17]. To assure a fair comparison of the proposed method and the other methods, the experiments were conducted under the same conditions. To obtain the best possible system response for each technique, the controller parameters for the PID, SMC, STLF, NFTSMC, and proposed methods were iteratively tuned to select the appropriate parameters by trial and error. Relevant parameters of the five control methods are given below. The parameters for the nonlinear observer gain were $L_1 = 900$ and $L_2 = 1.6$. The PID, SMC, STLF, and NFTSMC position controls were based on the cascade control structure. They consisted of the d and q inner PI current controllers. The control gains of the two PI controllers for the $d-$ and $q-$axis current loops were constructed using a cancellation approach [3]. The cutoff frequency of the current controls was 1000 Hz, and the current control gains were $k_p = 7$ and $k_i = 8796$. The parameters for the PID control were $k_{p,pos} = 64.5$, $k_{i,pos} = 738$, and $k_{d,pos} = 1$. The SMC position control [13] with sliding surface $S_3 = \dot{e}_0 + c_3 e_0$ and the reaching law $\dot{S}_3 = -k_5 sgn(S_3) - k_6 S_3$ was designed with the parameters

TABLE 1. System parameters for experiments.

Parameter	Value	Parameter	Value
Rated voltage	24 V	Limited current	±6.5 A
Rated speed	2500 rpm	Rated torque	0.12 N.m
Torque constant	0.0613 N.m/A	Pole pairs	5
J_n	$54\times10^{-6} kg.m^2$	L_q, L_d	1.13 mH
B_n	$1.2\times10^{-3} kg.m^2/s$	R	1.4 Ω

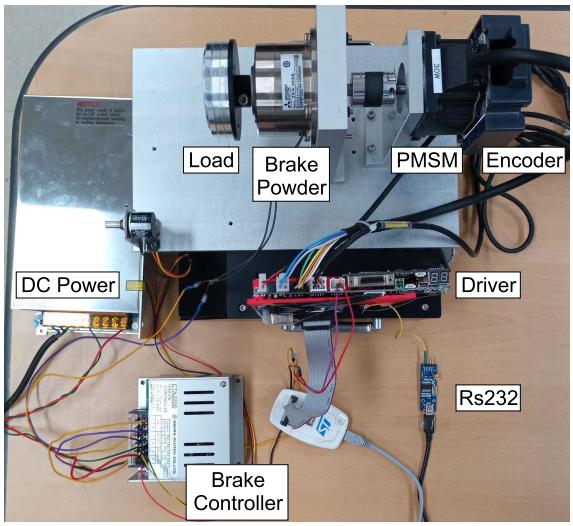

FIGURE 9. Experimental setup.

$c_3 = 300$, $k_5 = 15$, and $k_6 = 30$. The (STLF) controller [16] was configured such that $\alpha_{STLF} = 0.95$, $\beta_{STLF} = 30$, $\varepsilon_{STLF} = -0.05$. The (NFTSMC) [17] with $l_{NFTSMC} = 191$, $h_{NFTSMC} = 101$, $p_{NFTSMC} = 111$, $q_{NFTSMC} = 101$, $\alpha_{NFTSMC} = 0.1$, $\beta_{NFTSMC} = 0.01$, $\varepsilon_{NFTSMC} = 25$, $k_{1,NFTSMC} = 70$, $k_{2,NFTSMC} = 0.3$, $\delta_{NFTSMC} = 0.9$. The sampling frequency of the current loops was 20 kHz, and the position control loop was 2 kHz. The common parameters for the BSMC and ABSMC were $c_0 = c_1 = 180$, $\alpha_1 = 800$, $k_1 = k_3 = 700$, $k_2 = k_4 = 1500$. The adaptive parameters for ABSMC were $\lambda = 2.5$, $\eta = 0.5$, and the threshold $\delta = 2$.

The following results show the performance of the proposed ABSMC+NDO for position control when uncertainties and external load torque are taken into account. The real inertia of the system is $J_r = J_n + \Delta J = 111 \times 10^{-6} kg.m^2$. In this study, the proposed method was tested under the trapezoidal velocity motion profile as shown in Fig. 2, the step profile, and the sinusoidal profile to illustrate the effectiveness of the proposed method.

Fig. 10 shows the results of the PID+NDO, SMC+NDO, STLF, NFTSMC+NDO, and ABSMC+NDO. From Fig. 10(a) to 10(e), we can see that the ABSMC+NDO produced the best results, with a maximum position error of 0.008 rad, while the PID+NDO had a maximum error of 0.017 rad, the SMC+NDO had a maximum error of 0.021 rad, the STLF had a maximum error of 0.022 rad, and the NFTSMC had a maximum error of 0.022 rad. As mentioned above in Fig. 3, the ABSMC+NDO and BSMC+NDO performed

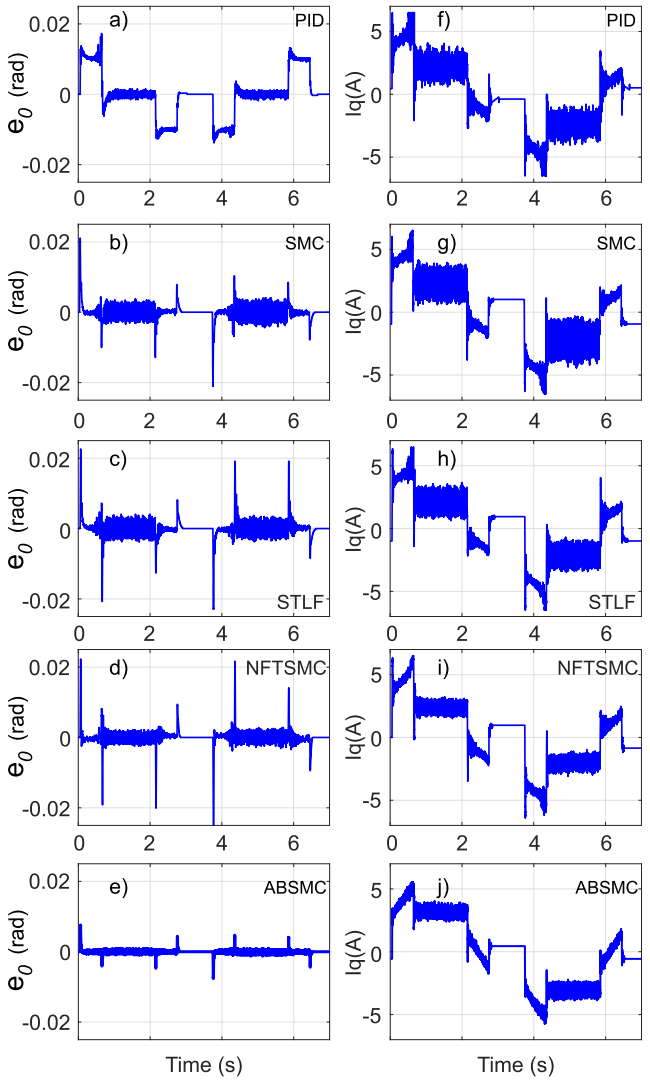

FIGURE 10. Performance comparison under a trapezoidal velocity motion profile, the steady-state speed is ± 2100 rpm. (a), (b), (c), (d), (e) Position error of PID+NDO, SMC+NDO, STLF, NFTSMC+NDO and the proposed ABSMC+NDO. (f), (g), (h), (i), (j) $q-$axis current of the PID+NDO, SMC+NDO, STLF, NFTSMC+NDO and the proposed ABSMC+NDO.

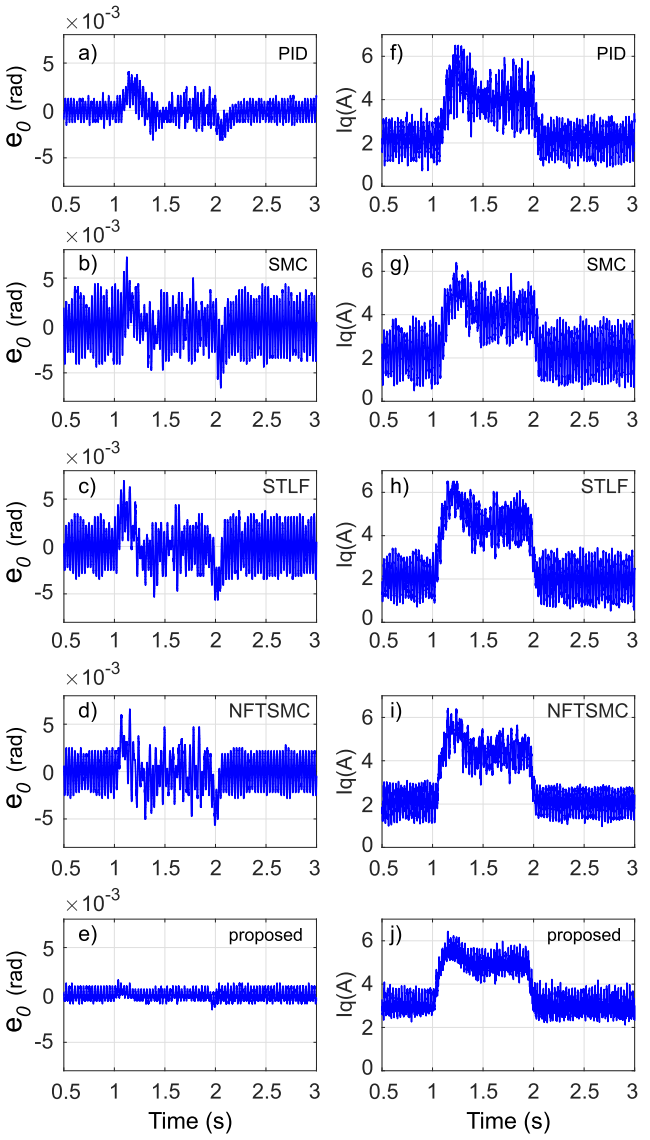

FIGURE 11. Performance comparison when the load torque occurs suddenly, the steady-state speed is 2100 rpm. (a), (b), (c), (d), (e) Position error of PID+NDO, SMC+NDO, STLF, NFTSMC+NDO and the proposed ABSMC+NDO. (f), (g), (h), (i), (j) $q-$axis current of the PID+NDO, SMC+NDO, STLF, NFTSMC+NDO and the proposed ABSMC+NDO.

similarly under trapezoidal velocity motion profiles. The main advantage of the ABSMC is the reduction of overshoot under the step position profile.

To depict the robustness of the proposed method under a sudden external load torque, the brake was controlled to produce an external load torque of 0.12 Nm at 1 s and release the load at 2 s. The position errors of the motor with the PID+NDO, SMC+NDO, STLF, NFTSMC+NDO, and the proposed ABSMC+NDO are shown in Fig. 11. The proposed ABSMC+NDO can produce superior disturbance rejection compared with the other methods in the event of a sudden external load torque.

Fig. 5 shows the results of the ABSMC+NDO and BSMC+NDO under the position step profile. As analyzed in Section V, the proposed ABSMC+NDO can reduce overshoot when compared with the BSMC+NDO. Fig. 12 shows the results of the PID+NDO, SMC+NDO, STLF, and NFTSMC+NDO when compared with the proposed ABSMC+NDO under the position step profile. As can be observed, the ABSMC+NDO achieved a faster settling time (0.27 s) compared with those of the PID+NDO (0.61 s), the SMC+NDO (0.61 s), the STLF (0.3 s), and the NFTSMC+NDO (0.39 s).

To test the performance of the ABSMC+NDO in a position step profile under an external load torque, an external load torque of 0.12 Nm was added during the step position profile, and the results are shown in Fig. 13. The ABSMC+NDO also had a shorter settling time (0.28 s) compared with the PID+NDO (0.72 s), SMC+NDO (0.67 s), the STLF (0.33 s),

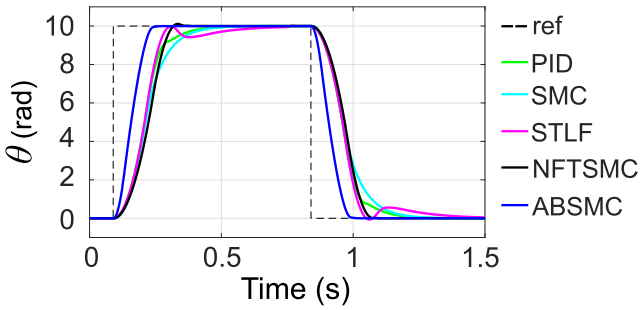

FIGURE 12. Performance comparison of PID+NDO, SMC+NDO, STLF, NFTSMC+NDO, and the proposed ABSMC+NDO under a point-to-point profile (step change 10*rad*).

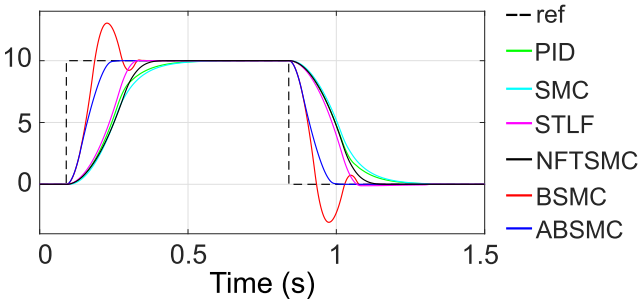

FIGURE 13. Performance comparison of Performance comparison of PID+NDO, SMC+NDO, STLF, NFTSMC+NDO, BSMC+NDO, and the proposed ABSMC+NDO under a point-to-point profile (step change 10*rad*, external load torque $T_L = 0.12$ *Nm*).

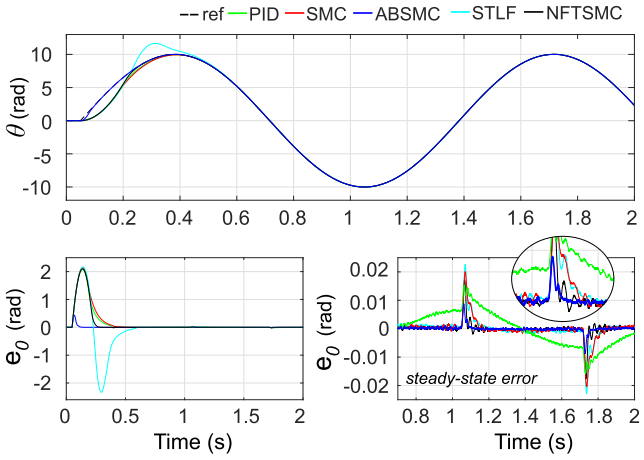

FIGURE 14. Performance comparison of PID+NDO, SMC+NDO, STLF, NFTSMC+NDO, and the proposed ABSMC+NDO under a sinusoidal profile with an external load torque $T_L = 0.12$ *Nm*. (a) Position tracking. (b) Position error. (c) Steady-state position error.

NFTSMC+NDO (0.42 s), and a smaller overshoot compared with the BSMC+NDO (30%).

Fig. 14 supplies the experimental results under the sinusoidal position profile of $10sin(1.5\pi t)$ with an external load torque of 0.12 Nm. The PID+NDO had the maximum error, settling time, and maximum steady state error results of 2.08 rad, 0.6 s, and 0.015 rad, respectively. The results for the SMC+NDO are 2.14 rad, 0.6 s, and 0.02 rad, respectively. The results for the STLF are 2.33 rad, 0.75 s, and 0.022 rad,

TABLE 2. Summary of results.

	PID	SMC	STLF	NFTSMC	ABSMC
Max error (condition 1)	0.017 rad	0.021 rad	0.022 rad	0.022 rad	**0.008** rad
settling time (condition 2)	0.61 s	0.61 s	0.3 s	0.39 s	**0.27** s
settling time (condition 3)	0.72 s	0.67 s	0.33 s	0.42 s	**0.28** s
settling time (condition 4)	0.6 s	0.6 s	0.75 s	0.31 s	**0.16** s
Max error (condition 4)	2.08 rad	2.14 rad	2.33 rad	2.1 rad	**0.43** rad
Max steady-state error (condition 4)	0.015 rad	0.02 rad	0.022 rad	0.017 rad	**0.009** rad

condition 1: Trapezoidal velocity motion profile. The results corresponding to Fig. 10.
condition 2: Point-to-point profile (step change 10 rad). The results corresponding to Fig. 12.
condition 3: Point-to-point profile (step change 10 rad, external load torque $T_L = 0.12Nm$). The results corresponding to Fig. 13.
condition 4: sinusoidal profile with an external load torque. The results corresponding to Fig. 14.

respectively. The results for the NFTSMC+NDO are 2.1 rad, 0.31 s, and 0.017 rad, respectively. While the proposed ABSMC+NDO had the best results (0.43 rad, 0.16 s, and 0.009 rad, respectively).

Table 2 summarizes the experimental results of the proposed ABSMC+NDO when compared with the PID+NDO, SMC+NDO, STLF, and NFTSMC+NDO. According to these results, the ABSMC+NDO method performed better than the PID+NDO, SMC+NDO, STLF, and NFTSMC+NDO.

VII. CONCLUSION

In this study, an effective method for improving the position response of a PMSM system was proposed based on an ABSMC and a NDO. The ABSMC position controller includes the BSMC and an adaptive convergence gain algorithm. The BSMC is a combination of backstepping and SMC that simplifies the control structure and improves the dynamic response of position tracking. An adaptive convergence gain algorithm was used to reduce the large overshoot position response when the motor operated under a point-to-point position profile. The NDO with a nonlinear observer gain function was proposed to estimate the uncertainty of parameters and external load torque and was used as feedforward compensation for the ABSMC. The stability of the composite control, ABSMC+NDO, is guaranteed by Lyapunov theory. The effectiveness of the proposed method was confirmed by experiments that demonstrated the proposed method can improve the overall performance of the PMSM control system in terms of fast transient response, small steady-state position error, reduced overshoot, and robustness against unknown disturbances when compared with PID, SMC, STLF, and NFTSMC position control methods.

REFERENCES

[1] X. Sun, Z. Shi, L. Chen, and Z. Yang, "Internal model control for a bearingless permanent magnet synchronous motor based on inverse system method," *IEEE Trans. Energy Convers.*, vol. 31, no. 4, pp. 1539–1548, Dec. 2016.

[2] X. Sun, L. Chen, and Z. Yang, "Overview of bearingless permanent-magnet synchronous motors," *IEEE Trans. Ind. Electron.*, vol. 60, no. 12, pp. 5528–5538, Dec. 2013.
[3] S. Yang and K. Lin, "Automatic control loop tuning for permanent-magnet AC servo motor drives," *IEEE Trans. Ind. Electron.*, vol. 63, no. 3, pp. 1499–1506, Mar. 2016.
[4] J. Yang, W.-H. Chen, S. Li, L. Guo, and Y. Yan, "Disturbance/uncertainty estimation and attenuation techniques in PMSM drives—A survey," *IEEE Trans. Ind. Electron.*, vol. 64, no. 4, pp. 3273–3285, Apr. 2017.
[5] T. Li, X. Liu, and H. Yu, "Backstepping nonsingular terminal sliding mode control for PMSM with finite-time disturbance observer," *IEEE Access*, vol. 9, pp. 135496–135507, 2021.
[6] W. Yin, X. Wu, and X. Rui, "Adaptive robust backstepping control of the speed regulating differential mechanism for wind turbines," *IEEE Trans. Sustain. Energy*, vol. 10, no. 3, pp. 1311–1318, Jul. 2019.
[7] F.-J. Lin, S.-G. Chen, and C.-W. Hsu, "Intelligent backstepping control using recurrent feature selection fuzzy neural network for synchronous reluctance motor position servo drive system," *IEEE Trans. Fuzzy Syst.*, vol. 27, no. 3, pp. 413–427, Mar. 2019.
[8] A. T. Nguyen, M. S. Rafaq, H. H. Choi, and J.-W. Jung, "A model reference adaptive control based speed controller for a surface-mounted permanent magnet synchronous motor drive," *IEEE Trans. Ind. Electron.*, vol. 65, no. 12, pp. 9399–9409, Dec. 2018.
[9] H. H. Choi, N. T.-T. Vu, and J.-W. Jung, "Digital implementation of an adaptive speed regulator for a PMSM," *IEEE Trans. Power Electron.*, vol. 26, no. 1, pp. 3–8, Jan. 2011.
[10] V. Q. Leu, H. H. Choi, and J.-W. Jung, "Fuzzy sliding mode speed controller for PM synchronous motors with a load torque observer," *IEEE Trans. Power Electron.*, vol. 27, no. 3, pp. 1530–1539, Mar. 2012.
[11] N. T.-T. Vu, D.-Y. Yu, H. H. Choi, and J.-W. Jung, "T–S fuzzy-model-based sliding-mode control for surface-mounted permanent-magnet synchronous motors considering uncertainties," *IEEE Trans. Ind. Electron.*, vol. 60, no. 10, pp. 4281–4291, Oct. 2013.
[12] T. H. Nguyen, T. T. Nguyen, V. Q. Nguyen, K. M. Le, H. N. Tran, and J. W. Jeon, "An adaptive sliding-mode controller with a modified reduced-order proportional integral observer for speed regulation of a permanent magnet synchronous motor," *IEEE Trans. Ind. Electron.*, vol. 69, no. 7, pp. 7181–7191, Jul. 2022.
[13] W. Gao and J. C. Hung, "Variable structure control of nonlinear systems: A new approach," *IEEE Trans. Ind. Electron.*, vol. 40, no. 1, pp. 45–55, Feb. 1993.
[14] S. Li, M. Zhou, and X. Yu, "Design and implementation of terminal sliding mode control method for PMSM speed regulation system," *IEEE Trans. Ind. Informat.*, vol. 9, no. 4, pp. 1879–1891, Nov. 2013.
[15] Q. Wang, H. Yu, M. Wang, and X. Qi, "An improved sliding mode control using disturbance torque observer for permanent magnet synchronous motor," *IEEE Access*, vol. 7, pp. 36691–36701, 2019.
[16] Q. Hou, S. Ding, X. Yu, and K. Mei, "A super-twisting-like fractional controller for SPMSM drive system," *IEEE Trans. Ind. Electron.*, vol. 69, no. 9, pp. 9376–9384, Sep. 2022.
[17] B. Xu, L. Zhang, and W. Ji, "Improved non-singular fast terminal sliding mode control with disturbance observer for PMSM drives," *IEEE Trans. Transport. Electrific.*, vol. 7, no. 4, pp. 2753–2762, Dec. 2021.
[18] T. T. Nguyen, H. N. Tran, T. H. Nguyen, and J. W. Jeon, "Recurrent neural network-based robust adaptive model predictive speed control for PMSM with parameter mismatch," *IEEE Trans. Ind. Electron.*, vol. 70, no. 6, pp. 6219–6228, Jun. 2023.
[19] Z. Mynar, L. Vesely, and P. Vaclavek, "PMSM model predictive control with field-weakening implementation," *IEEE Trans. Ind. Electron.*, vol. 63, no. 8, pp. 5156–5166, Aug. 2016.
[20] B. Xu, Q. Jiang, W. Ji, and S. Ding, "An improved three-vector-based model predictive current control method for surface-mounted PMSM drives," *IEEE Trans. Transport. Electrific.*, vol. 8, no. 4, pp. 4418–4430, Dec. 2022.
[21] M. Van, M. Mavrovouniotis, and S. S. Ge, "An adaptive backstepping nonsingular fast terminal sliding mode control for robust fault tolerant control of robot manipulators," *IEEE Trans. Syst., Man, Cybern., Syst.*, vol. 49, no. 7, pp. 1448–1458, Jan. 2018.
[22] J. Linares-Flores, C. Garcia-Rodriguez, H. Sira-Ramirez, and O. D. Ramirez-Cardenas, "Robust backstepping tracking controller for low-speed PMSM positioning system: Design, analysis, and implementation," *IEEE Trans. Ind. Informat.*, vol. 11, no. 5, pp. 1130–1141, Oct. 2015.
[23] Y. Tan, J. Chang, and H. Tan, "Adaptive backstepping control and friction compensation for AC servo with inertia and load uncertainties," *IEEE Trans. Ind. Electron.*, vol. 50, no. 5, pp. 944–952, Oct. 2003.
[24] Y. Wang, Y. Feng, X. Zhang, and J. Liang, "A new reaching law for antidisturbance sliding-mode control of PMSM speed regulation system," *IEEE Trans. Power Electron.*, vol. 35, no. 4, pp. 4117–4126, Apr. 2020.
[25] Z. Ma, Z. Liu, P. Huang, and Z. Kuang, "Adaptive fractional-order sliding mode control for admittance-based telerobotic system with optimized order and force estimation," *IEEE Trans. Ind. Electron.*, vol. 69, no. 5, pp. 5165–5174, May 2022.
[26] X. Zhang, L. Sun, K. Zhao, and L. Sun, "Nonlinear speed control for PMSM system using sliding-mode control and disturbance compensation techniques," *IEEE Trans. Power Electron.*, vol. 28, no. 3, pp. 1358–1365, Mar. 2013.
[27] F. Cupertino, D. Naso, E. Mininno, and B. Turchiano, "Sliding-mode control with double boundary layer for robust compensation of payload mass and friction in linear motors," *IEEE Trans. Ind. Appl.*, vol. 45, no. 5, pp. 1688–1696, Sep. 2009.
[28] F.-J. Lin, Y.-C. Hung, and K.-C. Ruan, "An intelligent second-order sliding-mode control for an electric power steering system using a wavelet fuzzy neural network," *IEEE Trans. Fuzzy Syst.*, vol. 22, no. 6, pp. 1598–1611, Dec. 2014.
[29] H. Dong, X. Yang, H. Gao, and X. Yu, "Practical terminal sliding-mode control and its applications in servo systems," *IEEE Trans. Ind. Electron.*, vol. 70, no. 1, pp. 752–761, Jan. 2023.
[30] J. Yang, S. Li, and X. Yu, "Sliding-mode control for systems with mismatched uncertainties via a disturbance observer," *IEEE Trans. Ind. Electron.*, vol. 60, no. 1, pp. 160–169, Jan. 2013.
[31] H. Pan, W. Sun, H. Gao, and X. Jing, "Disturbance observer-based adaptive tracking control with actuator saturation and its application," *IEEE Trans. Autom. Sci. Eng.*, vol. 13, no. 2, pp. 868–875, Apr. 2016.
[32] H. Pan and W. Sun, "Nonlinear output feedback finite-time control for vehicle active suspension systems," *IEEE Trans. Ind. Informat.*, vol. 15, no. 4, pp. 2073–2082, Apr. 2019.
[33] B. Fu, Q. Wang, and W. He, "Nonlinear disturbance observer-based control for a class of port-controlled Hamiltonian disturbed systems," *IEEE Access*, vol. 6, pp. 50299–50305, 2018.
[34] X. Liu, H. Yu, J. Yu, and Y. Zhao, "A novel speed control method based on port-controlled Hamiltonian and disturbance observer for PMSM drives," *IEEE Access*, vol. 7, pp. 111115–111123, 2019.
[35] L. Xu, G. Chen, and Q. Li, "Ultra-local model-free predictive current control based on nonlinear disturbance compensation for permanent magnet synchronous motor," *IEEE Access*, vol. 8, pp. 127690–127699, 2020.
[36] K.-S. Kim, K.-H. Rew, and S. Kim, "Disturbance observer for estimating higher order disturbances in time series expansion," *IEEE Trans. Autom. Control*, vol. 55, no. 8, pp. 1905–1911, Aug. 2010.
[37] Y. Liu, J. Gao, Y. Zhong, and L. Zhang, "Extended state observer-based IMC-PID tracking control of PMLSM servo systems," *IEEE Access*, vol. 9, pp. 49036–49046, 2021.
[38] W.-H. Chen, "Disturbance observer based control for nonlinear systems," *IEEE/ASME Trans. Mechatronics*, vol. 9, no. 4, pp. 706–710, Dec. 2004.
[39] W.-H. Chen, D. J. Ballance, P. J. Gawthrop, and J. O'Reilly, "A nonlinear disturbance observer for robotic manipulators," *IEEE Trans. Ind. Electron.*, vol. 47, no. 4, pp. 932–938, Aug. 2000.
[40] H. Liu and S. Li, "Speed control for PMSM servo system using predictive functional control and extended state observer," *IEEE Trans. Ind. Electron.*, vol. 59, no. 2, pp. 1171–1183, Feb. 2012.

TON HOANG NGUYEN received the B.S. degree in mechatronics engineering from the Ho Chi Minh City University of Technology, Ho Chi Minh City, Vietnam, in 2016, and the Ph.D. degree in electrical and computer engineering from Sungkyunkwan University, Suwon, South Korea, in 2022.

He is currently a Postdoctoral Researcher with the College of Information and Computer Engineering, Sungkyunkwan University. His research interests include signal processing, motion control, robotics, and embedded systems.

TY TRUNG NGUYEN received the B.S. degree in automatic control engineering from the Hanoi University of Science and Technology, Hanoi City, Vietnam, in 2018. He is currently pursuing the Ph.D. degree in electrical and computer engineering with the School of Information and Communication Engineering, Sungkyunkwan University, Suwon, South Korea.

His research interests include motion control, robotics, and embedded systems.

KIEN MINH LE received the B.S. degree in electrical engineering from the Hanoi University of Science and Technology, Hanoi, Vietnam, in 2006, the M.S. degree in automation from Le Quy Don Technical University, Hanoi, in 2011, and the Ph.D. degree in electronic and electrical engineering from Sungkyunkwan University, Suwon, South Korea, in 2017.

From 2018 to 2019, he was a Postdoctoral Researcher with the ICT HRD Institute for Future Value Creation, Sungkyunkwan University. He is currently a Lecturer with the Faculty of Control Engineering, Le Quy Don Technical University. His research interests include motion control, automation, and embedded systems.

HOANG NGOC TRAN received the B.S. degree in mechatronics engineering from the Ho Chi Minh City University of Technology, Ho Chi Minh City, Vietnam, in 2015, and the Ph.D. degree in electrical and computer engineering from Sungkyunkwan University, Suwon, South Korea, in 2020.

From 2020 to 2022, he was with the Department of Electrical and Computer Engineering, Sungkyunkwan University, as a Postdoctoral Researcher. Since 2022, he has been a Lecturer and a Researcher with the Department of Information Technology, FPT University, Can Tho, Vietnam. His research interests include signal processing, motion control, embedded systems, autonomous robotics, and machine learning.

JAE WOOK JEON (Senior Member, IEEE) received the B.S. and M.S. degrees in electronics engineering from Seoul National University, Seoul, South Korea, in 1984 and 1986, respectively, and the Ph.D. degree in electrical engineering from Purdue University, West Lafayette, IN, USA, in 1990.

From 1990 to 1994, he was a Senior Researcher with Samsung Electronics, Suwon, South Korea. Since 1994, he has been working as an Assistant Professor with the School of Electrical and Computer Engineering, Sungkyunkwan University, Suwon, where he is currently a Professor with the School of Information and Communication Engineering. His research interests include robotics, embedded systems, and factory automation.